The Haar–Wavelet Transform in Digital Image Processing: Its Status and Achievements

Piotr Porwik, Agnieszka Lisowska

Institute of Informatics, University of Silesia, ul. Będzińska 39, 41-200 Sosnowiec, Poland
e-mail: porwik@us.edu.pl
Institute of Mathematics, University of Silesia, ul. Bankowa 14, 40-007 Katowice, Poland
e-mail: alisow@ux2.math.us.edu.pl

Abstract. Image processing and analysis based on the continuous or discrete image transforms are classic techniques. The image transforms are widely used in image filtering, data description, etc. Nowadays the wavelet theorems make up very popular methods of image processing, denoising and compression. Considering that the Haar functions are the simplest wavelets, these forms are used in many methods of discrete image transforms and processing. The image transform theory is a well known area characterized by a precise mathematical background, but in many cases some transforms have particular properties which are not still investigated. This paper for the first time presents graphic dependences between parts of Haar and wavelets spectra. It also presents a method of image analysis by means of the wavelets–Haar spectrum. Some properties of the Haar and wavelets spectrum were investigated. The extraction of image features immediately from spectral coefficients distribution were shown. In this paper it is presented that two–dimensional both, the Haar and wavelets functions products man be treated as extractors of particular image features. Furthermore, it is also shown that some coefficients from both spectra are proportional, which simplify slightly computations and analyses.

Key words: Wavelets, Haar Transform, multiresolution.

1. Introduction

The computer and video–media applications have developed rapidly the field of multi-media, which requires the high performance, speedy digital video and audio capabilities. Nowadays, the image processing and analysis based on continuous or discrete transforms are the classic processing techniques [3, 27, 30, 36, 50]. Digital signal processing is widely used in many areas of electronics, communication and information techniques [1, 4, 6, 9, 14, 15, 17, 18, 20, 23, 28, 35]. In the signals compression, digital filtration, systems identification, the commonly used transforms are based on sinusoidal basic functions such as: Discrete Fourier Transform, Discrete Sine or Cosine Transform, Hartley Transform or rectangular basic functions Slant Transform, Discrete Walsh Transform, and Discrete Wavelet Transform (Haar, Daubechies, etc.) [3, 4, 6, 11, 12, 17, 25, 49, 50]. All these mentioned functions are orthogonal, and their forward and inverse transforms require only additions and subtractions. It makes that it is easy to implement them on the computer.

Haar functions are used since 1910. They were introduced by Hungarian mathematician Alfred Haar [1]. Nowadays, several definitions of the Haar functions and various generalizations [39] as well as some modifications [19, 37, 50] were published and used. One of the best modification, which was introduced, is the lifting scheme [25, 26, 29]. These transforms have been applied, for instance, to spectral techniques for multiple–valued logic, image coding, edge extraction, etc. Over the past few years, a variety of powerful and sophisticated wavelet–based schemes for image compression, as discussed later, were developed and implemented. Wavelet scheme gives many advantages, which are used in the JPEG–2000 standard as wavelet–based compression algorithms [31].

Generally, wavelets, with all generalizations and modifications, were intended to adapt this concept to some practical applications [40, 42]. The Discrete Wavelet Transform uses the Haar functions in image coding, edge extraction and binary logic design and is one of the most promising technique today. The non–sinusoidal Haar transform is the complete unitary transform [15, 16, 17]. It is local, thus can be used for data compression of non–stationary "spiky" signals. The digital images may be treated as such "spiky" signals. Unfortunately, the Haar Transform has poor energy compaction for image, therefore in practice, basic Haar transform is not used in image compression. One should remember that researches in this topic are still in progress and everyday new solutions and improvements are found [33, 39, 41, 43, 47].

Fourier methods are not always good tools to recapture the signal [3], particularly if it is highly non–smooth; too much Fourier information is needed to reconstruct the signal locally. In these cases the wavelet analysis is often very effective because it provides a simple approach for dealing with the local aspects of a signal, therefore particular properties of the Haar or wavelet transforms allow to analyse the original image on spectral domain effectively. These methods will be described in this paper.

2. The Discrete Haar Transform

A complete orthogonal system of functions in $L^p[0, 1]$, $p \in [0, \infty]$ which take values from the set $\{0, 2^j : j \in \mathbf{N}\}$ was defined by Haar [1]. This system of functions has property that each function continuous on interval $[0, 1]$ may be represented by a uniformly and convergent series in terms of elements of this system. Nowadays, in the literature, there are some other definitions of the Haar functions [16]. Those definitions are mutually differing with respect to the values of Haar functions at the points of discontinuity. For example the original Haar definition is as follows [4]:

$$haar(0, t) = 1, \text{ for } t \in [0, 1); \quad haar(1, t) = \begin{cases} 1, & \text{for } t \in [0, \frac{1}{2}), \\ -1, & \text{for } t \in [\frac{1}{2}, 1) \end{cases} \qquad (1)$$

and $haar(k, 0) = \lim_{t \to 0+} haar(k, t)$, $haar(k, 1) = \lim_{t \to 1-} haar(k, t)$ and at the points of discontinuity within the interior $(0, 1)$ $haar(k, t) = \frac{1}{2}(haar(k, t - 0) + haar(k, t + 0))$.

Instead of described relations some authors use the formula $haar(k,t) = haar(k, t + 0)$ where in the practice it is usually assumed that the Haar function takes zero value at the points of discontinuity.

Discrete Haar functions may be defined as functions determined by sampling the Haar functions at 2^n points. These functions can be conveniently represented by means of matrix form. The Haar matrices $\mathbf{H}(n)$ are considered in the natural and sequence ordering which differ in the ordering of rows. Each row of the matrix $\mathbf{H}(n)$ includes the discrete Haar sequence $haar(w,t)$ (or otherwise the discrete Haar function). In this notation, index w identifies the number of the Haar function and index t the discrete point of the function determination interval. In this case, the Haar matrix of any dimension may be obtained by the following recurrence relation [3]:

$$\mathbf{H}(n) = \begin{bmatrix} \mathbf{H}(n-1) & \otimes[1 \quad 1] \\ 2^{(n-1)/2}\mathbf{I}(n-1) & \otimes[1 \quad -1] \end{bmatrix}, \quad \mathbf{H}(0) = 1 \qquad (2)$$

and $\mathbf{H}(n) \neq \mathbf{H}(n)^T$ for $n > 1$ and $\mathbf{H}(n)^{-1} = 2^{-n} \cdot \mathbf{H}(n)^T$, where $\mathbf{H}(n)$ — matrix of the discrete Haar functions of degree 2^n, $\mathbf{I}(n)$ — identity matrix of degree 2^n, $\otimes$ — the Kronecker (tensor) product.

From (2) one can observe that, unlike the Fourier transform, $\mathbf{H}(n)$ matrix has only real elements. The Haar matrix is non–symmetric and its elements are 1, −1 or 0, multiplied by powers of $\sqrt{2}$. The discrete, orthogonal Haar functions, obtained from the formula (2), are defined on $[0, 1)$ interval.

Def. 2.1. Two–dimensional $N \times N = 2^n \times 2^n$ forward discrete Haar transform is defined in matrix notation as

$$\mathbf{S} = a \cdot \mathbf{H}(n) \cdot \mathbf{F} \cdot a \cdot \mathbf{H}(n)^T. \qquad (3)$$

The inverse transform is defined as

$$\mathbf{F} = b \cdot \mathbf{H}(n)^T \cdot \mathbf{S} \cdot b \cdot \mathbf{H}(n), \qquad (4)$$

where $\mathbf{F}$ is the image in matrix form, the matrix is of dimension $N \times N$ pixels, $\mathbf{S}$ is the spectrum matrix and $a \cdot b = 1/N$, hence parameters a or b may be defined as values $1/N$, $1/\sqrt{N}$ or 1, $n = \log_2 N$.

Because matrix (2) has many zero entries, some values of the Haar spectral coefficients are equal to 0 too. Fig. 1 presents some known transforms of a test image. As transform matrices $\mathbf{H}(n)$, Walsh–Hadamard, Haar, sine and cosine matrices were used. All figures make up the graphic representation of spectral coefficients. Therefore each picture in Fig. 1 may be interpreted as matrix, where axis *row* and *col* describe elements of matrix $\mathbf{S}$ and axis *value of coeff.* indicates values of spectral coefficients in $\mathbf{S}$. The test image $\mathbf{F}$ is built as 8×8 matrix, which has zero values everywhere except the upper left element, which has the value of eight.

The Fast Haar Transform has already been well known from many works [3, 4, 5, 17, 28] therefore it will not be present in details. The Haar transform is a symmetric,

separable transform that uses Haar function for its basis. It exists for $N = 2^n$, where n is an integer. The Haar function, which is an odd rectangular pulse pair, is the simplest and oldest orthonormal wavelet [16, 17, 28]. Whereas the Fourier transform basis functions differ only in frequency, the Haar functions vary in the both scales of width and position.
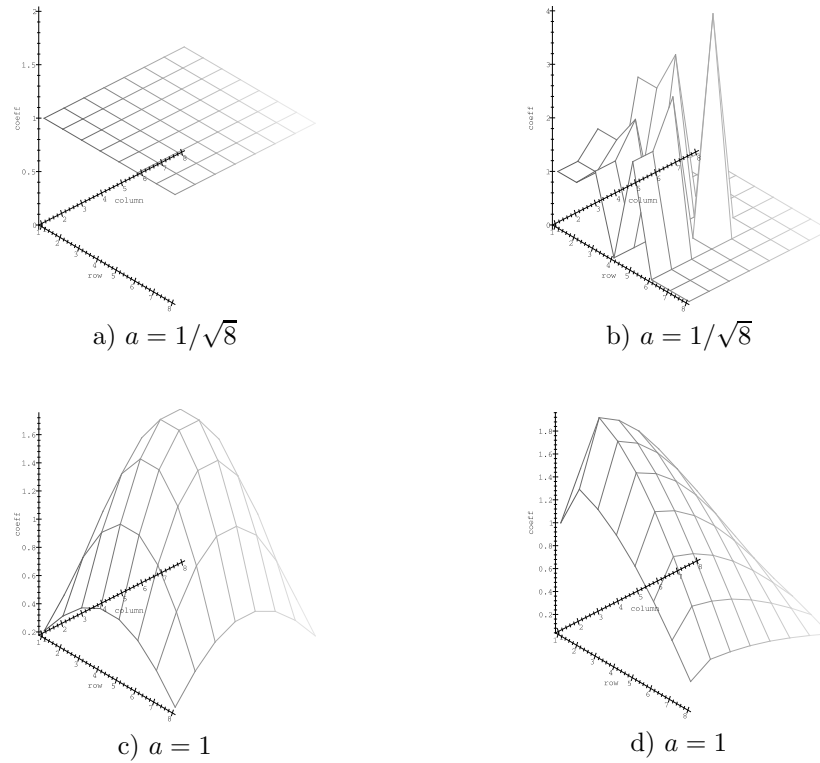

a) $a = 1/\sqrt{8}$ b) $a = 1/\sqrt{8}$

c) $a = 1$ d) $a = 1$

Fig. 1. The S transform of image containing the test impulse: a) Walsh–Hadamard, b) Haar, c) DST (Discrete Sine Transform), d) DCT (Discrete Cosine Transform).

From Fig. 1 we can observe that all N^2 elements of these transforms are nonzero except the Haar transform, which has only $2N$ nonzero entries. These features are very important in image processing because in many cases spectral coefficients have zero entries before next retrieval operations. This case occurs in black and white images very often. From image data compression point of view, this case is very convenient. From the energy distribution it can be estimated which spectral coefficients can be reduced [15, 17, 28]. It is easy to observe from Fig. 1 that the Walsh transform gives the worst results here: distribution of spectral energy is uniformable. In c) and d) cases distribution

of spectral energy has sharply outlined maximum. Outside of the maximum value, one can observe the decrease of energy. Unfortunately, the distribution of the Haar spectrum (Fig. 1b) is not proper too, but we can treat this transform differently.

The discrete transforms, presented in Fig. 1, enable us to observe where energy concentrations occur. Hence, we know which spectral coefficients are important in image processing. From this representation, it is not possible to find more precisely information about real image. For example, it is difficult to point places, which describe horizontal, vertical, etc. details of real image. These troubles can be overcome by well known multiresolution analysis [11, 17, 20, 34, 49].

3. The Discrete Haar Wavelet Transform

An outstanding property of the Haar functions is that except function $haar(0, t)$, the i–th Haar function can be generated by the restriction of the $(j - 1)$–th function to be half of the interval where it is different from zero, by multiplication with $\sqrt{2}$ and scaling over the interval $[0, 1]$. These properties give considerable interest of the Haar function, since they closely relate them to the wavelet theory. In this setting, the first two Haar functions are called the global functions, while all the others are denoted as the local functions. Hence, the Haar function, which is an odd rectangular pulse pair, is the simplest and oldest wavelet. The motivation for using the discrete wavelet transform is to obtain information that is more discriminating by providing a different resolution at different parts of the time–frequency plane. The wavelet transforms allow the partitioning of the time-frequency domain into nonuniform tiles in connection with the time–spectral contents of the signal. The wavelet methods are strongly connected with classical basis of the Haar functions; scaling and dilation of a basic wavelet can generate the basis Haar functions.

Def. 3.1. Let $\Psi: \mathbf{R} \to \mathbf{R}$, the Haar wavelet function is defined by the formula [43]:

$$\Psi(t) = \begin{cases} 1, & \text{for } t \in [0, \frac{1}{2}), \\ -1, & \text{for } t \in [\frac{1}{2}, 1), \\ 0, & \text{otherwise.} \end{cases} \tag{5}$$

Taking into account the Definition 3.1, any Haar function (except function $haar(0, t)$) from basis (2) may be generated by means of the formulas:

$$\Psi_i^j(t) = \sqrt{2^j}\Psi(2^j t - i), \qquad i = 0, 1, \ldots, 2^j - 1 \text{ and } j = 0, 1, \ldots, \log_2 N - 1. \tag{6}$$

The constant $\sqrt{2^j}$ is chosen so that the scalar product $< \Psi_i^j, \Psi_i^j >= 1$, $\Psi_i^j \in L^2(\mathbf{R})$. If one considers the wavelet function on other intervals than $[0, 1)$, the normalisation constant will be different. For example: $\Psi_0^0 = haar(1, t)$, $\Psi_0^1 = haar(2, t)$, $\Psi_1^1 = haar(3, t)$,

$\Psi_0^2 = haar(4,t)$, $\Psi_1^2 = haar(5,t)$, $\Psi_2^2 = haar(6,t)$, $\Psi_3^2 = haar(7,t)$. Generally $\Psi_i^j = haar(2^j + i, t)$. From this example follows that functions $\Psi_i^j(t)$ are orthogonal to one another. Hence, we obtain linear span of vector space $W^j = span\{\Psi_i^j\}_{i=0,\ldots,2^j-1}$. A collection of linearly independent functions $\{\Psi_i^j(t)\}_{i=0,\ldots,2^j-1}$ spanning W^j is called wavelets.

Def. 3.2. Let $\Phi\colon \mathbf{R} \to \mathbf{R}$, the Haar scaling function is defined by the formula [43]:

$$\Phi(t) = \begin{cases} 1, & \text{for } t \in [0,1), \\ 0, & \text{for } t \notin [0,1). \end{cases} \qquad (7)$$

Similarly to the properties of the wavelet function, for scaling function one can define the family of functions:

$$\Phi_i^j(t) = \sqrt{2^j}\,\Phi(2^j t - i), \qquad i = 0, 1, \ldots, 2^j - 1 \text{ and } j = 0, 1, \ldots, \log_2 N - 1. \qquad (8)$$

The constant $\sqrt{2^j}$ is chosen so that the scalar product $< \Phi_i^j, \Phi_i^j > = 1$, $\Phi_i^j \in L^2(\mathbf{R})$. The index j refers to dilation and index i refers to translation [11, 17]. Hence, we obtain linear span of vector space $V^j = span\{\Phi_i^j\}_{i=0,\ldots,2^j-1}$. The basic functions from the space V^j are called scaling functions.

In multiresolution analysis the Haar basis has important property: $V^j = V^{j-1} \oplus W^{j-1}$, where $\oplus$ stands for orthogonality of V^j and W^j spaces [16].

From Definitions 3.1 and 3.2 follows, that vector space W^j can be treated as the orthogonal complement of V^j in V^{j+1}. In other words, let W^j be the space of all functions in V^{j+1} that are orthogonal to all functions in V^j. Therefore, the basis functions Ψ_i^j of W^j together with the basis functions Φ_i^j of V^j form a basis for V^{j+1} and every basis function Ψ_i^j of W^j is orthogonal to every basis function Φ_i^j of V^j. From the properties of the Haar functions, described above, follows that basic wavelet is progressively narrowed (reduced in scale) by powers of two. Each smaller wavelet is then translated by increments equal to its width, so that the complete set of wavelets at any scale completely covers the interval. From mentioned equations one can conclude, that the basic wavelet is scaled down by powers of 2, but its amplitude is scaled up by powers of $\sqrt{2}$.

4. The Haar and Wavelet Basic Images

Due to its low computing requirements, the Haar transform has been mainly used for image processing and pattern recognition. From this reason two dimensional signal processing is an area of efficient applications of Haar transforms due to their wavelet–like structure.

Because $\mathbf{H}(n)$ and $\mathbf{H}(n)^T$ are the square matrices, their product is commutative, therefore equations (3) and (4) can be rewritten and expressed as:

$$s(k,m) = \sum_{x=0}^{N-1} \sum_{y=0}^{N-1} f(x,y) \times haar(k,x) \times haar(m,y) , \qquad (9)$$

$$f(x,y) = \sum_{k=0}^{N-1} \sum_{m=0}^{N-1} s(k,m) \times haar(k,x) \times haar(m,y) , \qquad (10)$$

where $\mathbf{S} = [s_{km}]$, $\mathbf{F} = [f_{xy}]$, $x,y,k,m \in \{0,1,\ldots,N-1\}$.

Basing on equation of analysis (3) we can conclude that in 2D spectral domain the values of coefficients depend on appropriate product of the two Haar functions. Fig. 2 presents an example of multiplication the arbitrary selected Haar functions.
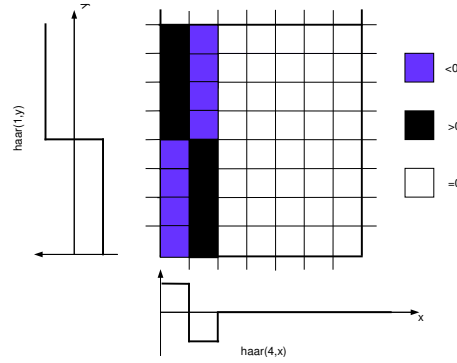

Fig. 2. The example of multiplication of the discrete Haar functions.

Because this product is multiplied by image matrix, the result of such multiplication may be treated as a particular extractor, which allows us to characterise the features in real image at specified point. In other words, that product can be used to locate the specific lines (edges) hidden in image. By looking for all coefficients in the spectral space, one can find all important edge directions in the image. This information can further be used in image (object) analysis [10].

Taking into account the Mallat algorithm [7, 8, 9] multiresolution image analysis can be applied to the classical Haar basis, described by matrix–equation (2). In this case, we must find decomposition matrices of matrix . Based on Fig. 2, construction of decomposition matrices can be as follows:

Step 1. According to the formula $V^n = V^{n-1} \oplus W^{n-1}$, the matrix $\mathbf{M}_1$ has a form

$$\mathbf{M}_1 = [\Phi_{j=0,\ldots,2^{n-1}-1}^{n-1} \subset V^{n-1}, \Psi_{j=0,\ldots,2^{n-1}-1}^{n-1} \subset W^{n-1}]^T .$$

Step 2. In second step, because $V^{n-1} = V^{n-2} \oplus W^{n-2} \oplus W^{n-1}$, the matrix $\mathbf{M}_2$ can be constructed as follows

$$\mathbf{M}_2 = [\Phi^{n-2}_{j=0,\dots,2^{n-2}-1} \subset V^{n-2}, \Psi^{n-2}_{j=0,\dots,2^{n-2}-1} \subset W^{n-2}, \Psi^{n-1}_{j=0,\dots,2^{n-1}-1} \subset W^{n-1}]^T .$$

...

Step n. Finally, after n steps of calculations $V^1 = V^0 \oplus W^0 \oplus W^1 \oplus W^2 \oplus \dots \oplus W^{n-1}$, hence the matrix $\mathbf{M}_n$ has a structure

$$\mathbf{M}_n = [\Phi^0_0 \subset V^0, \Psi^0_0 \subset W^0, \Psi^1_{j=0,1} \subset W^1, \dots, \Psi^{n-1}_{j=0,\dots,2^{n-1}-1} \subset W^{n-1}]^T .$$

Exmp. 4.1. Let $n = 3$ then:
$V^3 = V^2 \oplus W^2$

$$\mathbf{M}_1 = [\Phi^2_0, \Phi^2_1, \Phi^2_2, \Phi^2_3, \Psi^2_0, \Psi^2_1, \Psi^2_2, \Psi^2_3]^T =$$

$$\begin{bmatrix}
2 & 2 & 0 & 0 & 0 & 0 & 0 & 0 \\
0 & 0 & 2 & 2 & 0 & 0 & 0 & 0 \\
0 & 0 & 0 & 0 & 2 & 2 & 0 & 0 \\
0 & 0 & 0 & 0 & 0 & 0 & 2 & 2 \\
2 & -2 & 0 & 0 & 0 & 0 & 0 & 0 \\
0 & 0 & 2 & -2 & 0 & 0 & 0 & 0 \\
0 & 0 & 0 & 0 & 2 & -2 & 0 & 0 \\
0 & 0 & 0 & 0 & 0 & 0 & 2 & -2
\end{bmatrix}$$

$V^2 = V^1 \oplus W^1 \oplus W^2$

$$\mathbf{M}_2 = [\Phi^1_0, \Phi^1_1, \Psi^1_0, \Psi^1_1, \Psi^2_{j=0,\dots,3} \subset W^2]^T =$$

$$\begin{bmatrix}
\sqrt{2} & \sqrt{2} & \sqrt{2} & \sqrt{2} & 0 & 0 & 0 & 0 \\
0 & 0 & 0 & 0 & \sqrt{2} & \sqrt{2} & \sqrt{2} & \sqrt{2} \\
\sqrt{2} & \sqrt{2} & -\sqrt{2} & -\sqrt{2} & 0 & 0 & 0 & 0 \\
0 & 0 & 0 & 0 & \sqrt{2} & \sqrt{2} & -\sqrt{2} & -\sqrt{2} \\
2 & -2 & 0 & 0 & 0 & 0 & 0 & 0 \\
0 & 0 & 2 & -2 & 0 & 0 & 0 & 0 \\
0 & 0 & 0 & 0 & 2 & -2 & 0 & 0 \\
0 & 0 & 0 & 0 & 0 & 0 & 2 & -2
\end{bmatrix}$$

$V^1 = V^0 \oplus W^0 \oplus W^1 \oplus W^2$

$$\mathbf{M}_3 = [\Phi^0_0, \Psi^0_0, \Psi^1_{j=0,1} \subset W^1, \Psi^2_{j=0,\dots,3} \subset W^2]^T =$$

$$
\begin{bmatrix}
1 & 1 & 1 & 1 & 1 & 1 & 1 & 1 \\
1 & 1 & 1 & 1 & -1 & -1 & -1 & -1 \\
\sqrt{2} & \sqrt{2} & -\sqrt{2} & -\sqrt{2} & 0 & 0 & 0 & 0 \\
0 & 0 & 0 & 0 & \sqrt{2} & \sqrt{2} & -\sqrt{2} & -\sqrt{2} \\
2 & -2 & 0 & 0 & 0 & 0 & 0 & 0 \\
0 & 0 & 2 & -2 & 0 & 0 & 0 & 0 \\
0 & 0 & 0 & 0 & 2 & -2 & 0 & 0 \\
0 & 0 & 0 & 0 & 0 & 0 & 2 & -2
\end{bmatrix}
$$

For last decomposition level, it can be noticed that $\mathbf{M}_n = \mathbf{H}(n)$. If each orthogonal matrix $\mathbf{M}_i$, $i = 1, 2, 3$ will be multiplied by $1/\sqrt{2}$ factor, then the procedure of calculations will be according to the classical Mallat algorithm.

The product of the decomposition levels for all 2D Haar functions (for case $N = 8$) is shown in Fig. 3. Taking into account equation (9), these products can be treated as extractors of image features.
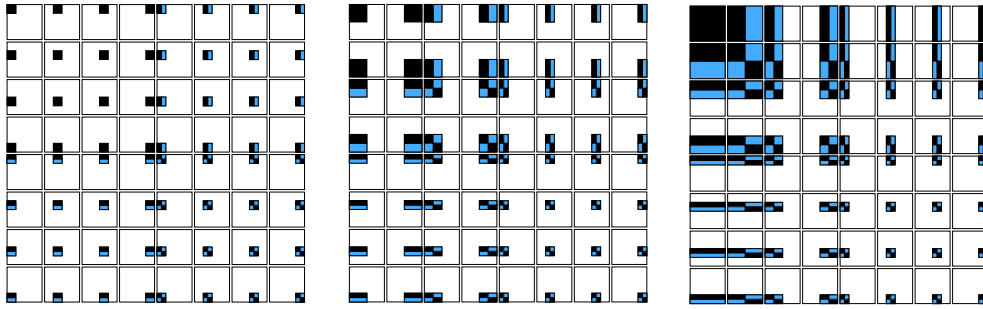

Fig. 3. The 2D Haar functions product treated as extractors. Decomposition levels: (left) first, (center) second, (right) third.

The pictures presented in Fig. 3 have been composed on the basis of $\mathbf{M}_i$, $i = 1, 2, 3$ matrices and method shown in Fig. 2.

From Fig. 3 we can conclude that the classical Haar transform gives different spectral coefficients on different decomposition levels. One advantage of the method presented above is that often a large number of the detail coefficients turn out to be very small in magnitude, as in the example of Fig. 1. Truncating, or removing, these small coefficients from the representation introduces only small errors in the reconstructed image, giving a form of lossy image compression. Additionally, we can control which coefficients will be removed, because its distribution is known (Fig. 3). In other words, that distribution

may be used to locate the specific lines (edges) hidden in image. By looking for all large coefficients in the spectral space, it can be found all important edge directions in the image.

There are many ways of forming the Haar spectrum. The simplest method consists of multiplying the data by the Haar matrices, then setting some of the resulting coefficients equal to zero (Fig. 1). A widely used method involves the specifying threshold [12, 15, 17]. All coefficients whose magnitudes lie bellow this threshold are set equal to 0. This method is frequently used for noise removal, where coefficients whose magnitudes are significant only, because of the added noise will often lie bellow a well–chosen threshold [15]. A second method keeps only the largest magnitude coefficients, while setting the rest equal to zero. This method is convenient for making comparison when it is known in advance how many terms are needed. A third method is called the energy method [15, 17]. This one involves specifying a fraction of the signal's energy, where the energy is the square root of the sum of squares of the coefficients. Then we retain the least number of the largest magnitude coefficients whose energy exceeds this fraction of the signal's energy and set all other coefficients equal to 0. Instead of the above–described methods of forming the Haar spectrum, we can apply the presented in this paper method of the 2D Haar function analysis. This new method allows very often obtaining the similar results through selection of the appropriate coefficients.

Problem of image analysis described above can be solved differently by applying the same functions and spaces. As it is known, there are two ways of forming the Haar coefficients: standard and non–standard method [16]. The standard approach has been presented above. In this paper is applied non–standard method because, as it will be shown, it has a strong connection with method of the Haar functions analysis described above. Additionally, non–standard method is slightly more efficient to compute spectral coefficients [49].

Basing on Definitions 3.1 and 3.2, on properties of the Haar functions and the facts that $V^j = span\{\Phi_i^j\}_{i=0,...,2^j-1}$, $W^j = span\{\Psi_i^j\}_{i=0,...,2^j-1}$ we can express functions Φ and Ψ as a linear combination of the basis functions from V and W spaces respectively. In the Haar wavelet case Φ and Ψ functions can be written as

$$\Phi(t) = h(0)\sqrt{2}\Phi(2t) + h(1)\sqrt{2}\Phi(2t-1)\,, \tag{11}$$

$$\Psi(t) = g(0)\sqrt{2}\Phi(2t) + g(1)\sqrt{2}\Phi(2t-1)\,, \tag{12}$$

where $\{h(0), h(1)\}$ and $\{g(0), g(1)\}$ define the low–pass and high–pass filters respectively. For this case, $h(k)$, $k = 0, 1$ coefficients are known [5]:

$$h(0) = \frac{1}{\sqrt{2}}\ , h(1) = \frac{1}{\sqrt{2}}\ , g(0) = \frac{1}{\sqrt{2}}\ , g(1) = -\frac{1}{\sqrt{2}}\ . \tag{13}$$

Let us denote **F** as an image in matrix form and define the operators

$$\mathbf{A}(i) = \frac{1}{\sqrt{2}}\mathbf{F}(2i) + \frac{1}{\sqrt{2}}\mathbf{F}(2i+1), \tag{14}$$

$$\mathbf{D}(i) = \frac{1}{\sqrt{2}}\mathbf{F}(2i) - \frac{1}{\sqrt{2}}\mathbf{F}(2i+1), \tag{15}$$

where $\mathbf{F}(i)$ — vector of size N, containing row or column of matrix $\mathbf{F}$, $i \in \{0, 1, \ldots, \frac{N}{2} - 1\}$, $\mathbf{A}(i)$ — vector of size $N/2$, containing approximation coefficients, $\mathbf{D}(i)$ — vector of size $N/2$, containing detail coefficients.

To get non–standard wavelet decomposition on the first level of an image $\mathbf{F}$ (the spectrum matrix called S_1) we first apply the operators (14), (15) to all columns of the matrix and then to all rows [16]. To get the second level of non–standard decomposition (that is matrix S_2) one can apply similar analysis to upper left sub–matrix of size $\frac{N}{2} \times \frac{N}{2}$ of matrix S_1. And generally, to get k–th level — matrix S_k, one can apply this analysis to upper left sub–matrix of size $\frac{N}{2^{k-1}} \times \frac{N}{2^{k-1}}$ of matrix S_{k-1}, where $k \in \{1, \ldots, \log_2 N\}$.

Note, that applying filters (14), (15) to an image, give the same results as multiplying matrices $S_1 = \frac{1}{8}\mathbf{M}_1 \cdot \mathbf{F} \cdot \mathbf{M}_1^T$, where matrix $\mathbf{M}_1$ is taken from Ex. 4.1. Therefore, S_1 may be treated as extractor of image features on the first level of wavelet decomposition, similar as above in Haar decomposition case. Because on the second and next levels only the part of a matrix is transformed (opposite to Haar decomposition) these extractors on these levels are different. For example, for $N = 8$ the products of the non–standard wavelet decomposition levels are shown in Fig. 4.
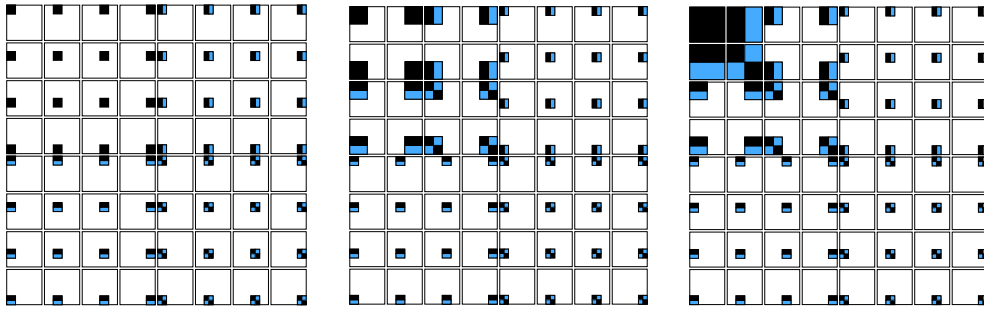

Fig. 4. The 2D wavelet functions product treated as extractors. Decomposition levels: (left) first, (center) second, (right)third.

All considerations, which have been presented until now for the classical of Haar functions, have applications in that case too, with the exception of extractors distribution (Fig. 4). Additionally, it is common knowledge that coefficients $h(k)$, $k = 0, 1$ (in other

words so–called filters) may be described by means of scalar product of functions Φ and Ψ respectively:

$$h(k) = < \Phi(t), \sqrt{2}\Phi(2t - k) > \tag{16}$$

$$g(k) = < \Psi(t), \sqrt{2}\Psi(2t - k) > \tag{17}$$

Presented both the standard and non–standard approaches are applied very often in practical solutions [5, 15, 16, 17, 28, 46]. Each of them has some advantages. The standard decomposition can be simply implemented as matrix multiplication. This presents equation (3). The non–standard algorithm is a bit more efficient. More compact description of the non–standard method allows us even increase efficient computation.

5. Experimental Results

In order to test Haar matrix–based method and wavelet approach the well known image–benchmarks were used. Mentioned benchmarks one can find in many databases. As test images we used some standard images such as Barbara, Bridge, Lena, Flowers, Mandrill, Baboon etc. Each of these images was of size $a \times a \times 8$ bits, where $a \in \{32, 64, 128, 256\}$, respectively.

By analysing the Figs. 3–4 we can divide area of each figure into 4 sub–sampled spaces. Each piece has dimension $(N/2) \times (N/2)$ and is called A, H, V and D respectively. Location of these sub–areas presents Fig 5.
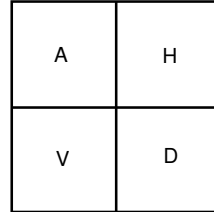

Fig. 5. Principle of spectra partitioning.

Each mentioned piece (A, H, V or D) for $N = 8$ includes sixteen (4×4) appropriate sub–squares from Fig. 3–4. According to presented previously arguments, mentioned areas possesses different features: A (Approximation Area) — includes information about the global properties of analysing image. Removing spectral coefficients from this area leads to the biggest distortion in origin image. H (Horizontal Area) — includes information about the vertical lines hidden in image. Removing spectral coefficients from this

area excludes horizontal details from origin image. V (Vertical Area) — contains information about the horizontal lines hidden in image. Removing spectral coefficients from this area eliminates vertical details from origin image. D (Diagonal Area) — embraces information about the diagonal details hidden in image. Removing spectral coefficients from this area leads to the smallest distortions in origin image.

Fig. 6 presents Baboon — the one of $256 \times 256 \times 8$ grey–level test images together with its wavelet and Haar spectra. The spectra images are different what directly follows from Figs. 3–4. Taking into account mentioned above features of areas some differences between spectres can be shown.
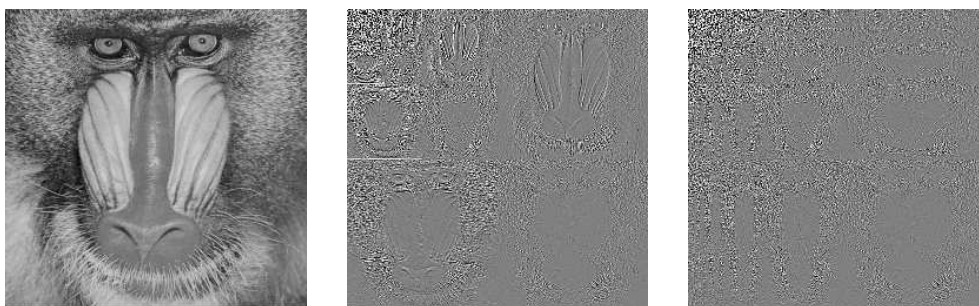

Fig. 6. Original image and its wavelet and Haar spectra, respectively.

Each left image from Figs. 7–10 presents place where spectrum was reduced. In this place, all spectral coefficients equal to zero. Two remained images show differences between origin image and the compressed one for wavelet and Haar method of analysis respectively.

Fig. 7. Horizontal details elimination and lost information after applied wavelet and Haar matrix–based method, respectively.

Fig. 8. Vertical details elimination and lost information after applied wavelet and Haar matrix–based method, respectively.

Fig. 9. Diagonal details elimination and lost information after applied wavelet and Haar matrix–based method, respectively.
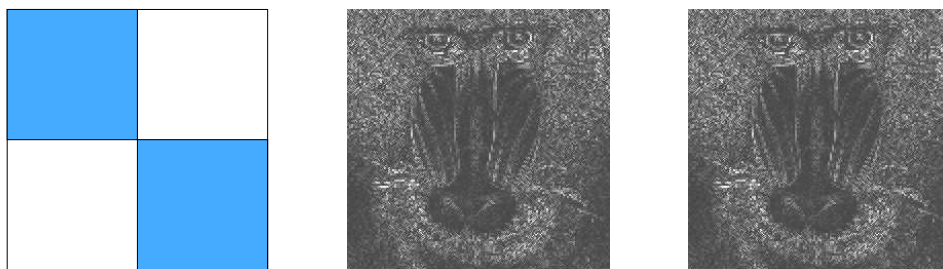

Fig. 10. Horizontal and vertical details elimination and lost information after applied wavelet and Haar matrix–based method, respectively.

The other cases of removing the spectral coefficients can be applied as well. These entire processes base on the fact, that appropriate selection and modification of the spectral coefficients may preserve the contents of the image. Depending on our needs we can shape compression ratio by means of natural selection of spectral coefficients directly from areas A, H, V, D or from their combinations. The exact information about distribution of spectral coefficients allows us to match easily up the compression ratio with the type of image, but this problem was not considered in the paper. In particular cases it is possible to obtain the large image compression ratio. Obtained results for Haar matrix–based method and wavelet method were compared by means of PSNR coefficients (hence there are some other similarity coefficients, for example like in [45]). These results of investigations are collected in Table 1. From this table one can see that Haar reconstructed images have slightly better quality.

Method	Horizontal (H)	Vertical (V)	Diagonal (D)	Horiz.+Vert. (H+V)
Wavelet decomp.	$29,7254$	$27,3697$	$31,4822$	$25,3813$
Haar decomp.	$29,7269$	$27,3702$	$31,4827$	$25,3813$

Tab. 1. The PSNR of reconstructed images after appropriate details elimination.

Between Haar matrix–based method and wavelet approach the quantitative and graphic relationship may be observed. Fig. 11 presents those relations. The image from Fig. 11 was constructed as a quotient between wavelet and Haar spectra respectively. These relationships will be obviously identical for any image objects.
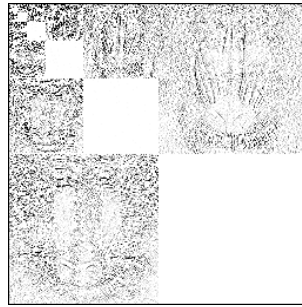

Fig. 11. Areas of the proportional coefficients (white squares) for Haar and wavelet spectres.

Moreover, it can be proven that for all diagonal coefficients on all levels of decomposition the following proposition is true.

Propos. 5.1. Let d_H stands for diagonal coefficients from Haar spectrum matrix and d_W stands for diagonal coefficients from wavelet spectrum matrix, both of degree 2^n. Then

$$d_H = 2^n d_W \,. \tag{18}$$

The proof of this fact, describing graphic dependences, follows instantly from Figs. 3–4 and arguments mentioned above, as well as appropriate proportionality of sub–matrices from the Haar and wavelet matrices on the same levels of decomposition.

This relationship is well visible in Fig. 11. The white areas appear just due to the proportionality of diagonal coefficients. Furthermore, note from Table 1 (the last column), that after removing all horizontal and vertical details on the first level of decomposition we get exactly the same PSNR of both methods reconstructed images because of the proportionality of the diagonal detail coefficients.

The amount of proportional coefficients can be easily computed. It is easy to see that the number of diagonal detail coefficients in spectrum matrix of size $2^n \times 2^n$ equals $\sum_{i=0}^{n-1} 2^i \cdot 2^i$. Hence, after simple calculations we get the following corollary.

Corollary 5.1. The number of proportional coefficients in Haar and wavelet matrices of size $2^n \times 2^n$ equals

$$\frac{\sum_{i=0}^{n-1} 2^i \cdot 2^i}{2^n \cdot 2^n} \approx \frac{1}{3} \,. \tag{19}$$

It means that as much as $1/3$ of all Haar matrix coefficients are proportional to wavelet matrix coefficients; for all of them the formula (18) is true.

6. Concluding Remarks

Wavelets analysis is a particular time–space scale representation of signals, which has found a wide range of applications in physics, signal processing and applied mathematics in the last years. The purpose of this paper was to compare the wavelets and the Haar functions in two–dimensional space. In many cases, these methods are similar. Presented in this paper the Haar matrix–based method and wavelet analysis can be used in many areas of image processing such as denoising, edge detection, edge preserving smoothing or filtering. In the paper is shown the graphic way of presentation of decomposition levels for both the Haar matrixbased method and wavelets. As it was shown both methods may be modelled on the basis of the wavelets theorem.

The 2D Haar matrix method of calculations like the 2D Fast Fourier Transform has complexity $O(4N^2 \log_2 N)$ [14], classical 2×1D fast non–standard wavelet method of calculations has complexity $O(16/3N^2)$ only [28]. This complexity can be decreased to $O(14/3N^2)$ by suitable organization of calculations [49]. Described complexity factors are determined as number of additions and multiplications in computation process. The graphic distribution of the Haar–wavelet spectral coefficients also was presented. Additionally, graphic presentation of spectra distribution allows us to point appropriate

selection or modification (reduction) of the Haar–wavelet coefficients. For example it may be removed vertical, horizontal or diagonal details of a given image.

The authors believe that this survey and problem description can be useful to researchers working in different disciplines where the discrete Haar and wavelets transforms are used.

References

1910

[1] Haar A.: Zur Theorie der orthogonalen Funktionensysteme. Mathematische Annalen, 69, 331–371.

1973

[2] Rudin W.: Functional Analysis. McGraw–Hill, New York.

1975

[3] Ahmed N., Rao K.R.: Orthogonal Transforms for Digital Signal Processing. Springer–Verlag, Berlin.

1977

[4] Harmuth H.F.: Sequency Theory. Foundations and applications. Academic Press, New York.

1978

[5] Pratt W. K.: Digital Image Processing. John Wiley and Sons, New York.

1988

[6] Besslich P. W., Trachtenberg L. A.: The sign transform an invertible non–linear transform with quantized coefficients. In: Moraga C., editor, Theory and application of spectral techniques, University Dortmund Press.

[7] Jain A.K.: Fundamentals of Digital Image Processing. Prentice Hall.

1989

[8] Mallat S.: Multifrequency channel decompositions of images and wavelet models. IEEE Transaction in Acoustic Speech and Signal Processing, 37, 2091–2110.

[9] Mallat S. A.: Theory for Multiresolution Signal Decomposition: The Wavelet Representation. IEEE Transactions on Pattern Analysis and Machine Intelligence, 11(7), 674–693.

[10] Yankowitz D., Bruckstein A.M.: A New Method for Image Segmentation. Computer Vision, Graphics and Image Processing, 46/1, 82–95.

1992

[11] Daubechies I.: Ten lectures on wavelets. Philadelphia PA, SIAM.

[12] Gröchenig K., Madych W. R.: Multiresolution Analysis, Haar bases and self–similar tilings of $\mathbf{R}^n$. IEEE Transactions on Information Theory, 38(2), 556–568.

1994

[13] Odegard J.: Image Enhancement by Nonlinear Wavelet Processing. Rice University CML Technical Report.

1995

[14] Bhaskaran V., Konstantinides K.: Image and video compression standards: algorithms and architectures. Kluwer, Boston.

[15] Stollniz E. J., DeRose T. D., Salesin D. H.: Wavelets for Computer Graphics: A Primer, Part 1. IEEE Computer Graphics and Applications, 76–84.

[16] Fournier A.: Wavelets and their Applications in Computer Graphics. SIGGRAPH'95 Course Notes, University of British Columbia.

1996

[17] Castleman K. R.: Digital Image Processing. Prentice–Hall, New Jersey.

1997

[18] Calderbank A. R., Daubechies I., Sweldens W., Yeo B. L.: Lossless image compression using integer to integer wavelet transforms. Proceedings of the International Conference on Image Processing, 1, 596–599.

[19] Claypoole R., Davis G., Sweldens W., Baraniuk R.: Adaptive Wavelet Transforms for Image Coding. Asilomar Conference on Signals, Systems and Computers.

[20] Creusere C. D.: A new method of robust image compression based on the embedded zerotree wavelet algorithm. IEEE Transactions on Image Processing, 6, 1436–1442.
[21] Przelaskowski A., Kazubek M., Jamrógiewicz T.: Optimalization of the Wavelet–Based Algorithm for Increasing the Medical Image Compression Efficiency. Proceedings of the TFTS'97 — 2nd IEEE UK Symposium on Applications of Time–Frequency and Time–Scale Methods, 177-180.
[22] Walker J. S.: Fourier Analysis and Wavelet Analysis. Notices of the American Mathematical Society, 44(6), 658–670.
[23] Wojtaszczyk P.: A Mathematical Introduction to Wavelets. Cambridge University Press, Cambridge.

1998
[24] Calderbank A. R., Daubechies I., Sweldens W., Yeo B. L.: Wavelet transforms that map integers to integers. Applied and Computational Harmonics Analysis, 5(3), 332–369.
[25] Daubechies I.: Recent results in wavelet applications. Journal of Electronic Imaging, 7(4), 719–724.
[26] Daubechies L., Sweldens W.: Factoring wavelet transforms into lifting steps. J. Fourier Anal. Appl., 4(3), 247–269.
[27] Davis G., Nosratinia A.: Wavelet–Based Image Coding: An Overview. Applied and Computational Control, Signals, and Circuits, 1(1).
[28] Sonka M., Hlavac V., Boyle R.: Image processing, Analysis and Machine Vision. Brooks/Cole Publishing Comp.

1999
[29] Davis G., Strela V., Turcajova R.; Multivwavelet Construction via the Lifting Scheme. Wavelet Analysis and Multiresolution Methods, T. X. He (editor), Lecture Notes in Pure and Applied Mathematics, Marcel Dekker.
[30] Smith S. W.: The Scientist and Engineer's Guide to Digital Signal Processing. California Technical Publishing, San Diego.

2000
[31] Christopoulos C., Skodras A., Ebrahimi T.: The JPEG2000 Still Image Coding System: an Overview. IEEE Transactions on Consumer Electronics, 46(4), 1103–1127.
[32] Fernandes F., van Spaendonck R., Burrus C.: Directional Complex–Wavelet Processing. Wavelet Applications in Signal and Image Processing.
[33] Jahromi O. S., Francis B. A., Kwong R. H.: Algebraic theory of optimal filterbanks. Proceedings of IEEE International Conference on Acoustics, Speech and Signal Processing, 1, 113–116.
[34] Romberg J., Choi H., Baraniuk R., Kingsbury N.: Multiscale Classification using Complex Wavelets. IEEE International Conference on Image Processing, Vancouver, Canada.

2002
[35] Addison P. S., Watson J. N., Feng T.: Low–Oscillation Complex Wavelets. Journal of Sound and Vibration, 254(4), 733–762.
[36] Blu T., Unser M.: Wavelets, Fractals and Radial Basis Functions, IEEE Transactions on Signal Processing, 50(3), 543–553.
[37] Munoz A., Ertle R., Unser M.: Continuous wavelet transform with arbitrary scales and $O(N)$ complexity. Signal Processing, 82, 749–757.
[38] Resnikoff H., Wells R. O. Jr.: Wavelet Analysis. Springer–Verlag, New York.
[39] Zeng L., Jansen C. P., Marsch S., Unser M., Hunziker R.: Four–Dimensional Wavelet Compression of Arbitrarily Sized Echocardiographic Data. IEEE Transactions on Medical Imaging, 21(9), 1179–1188.

2003
[40] Drori I., Lischinski D.: Fast Multiresolution Image Operations in the Wavelet Domain. IEEE Transactions on Visualization and Computer Graphics, 9(3), 395–411.
[41] Fernandes F., Selesnick I., van Spaendonck R., Burrus C.: Complex Wavelet Transforms with Allpass Filters. Signal Processing, 83(8), 1689–1706.
[42] Jorgensen P.: Matrix Factorizations, Algorithms, Wavelets. Notices of the American Mathematical Society, 50(8), 880–894.
[43] Jahromi O. S., Francis B. A., Kwong R. H.: Algebraic theory of optimal filterbanks. IEEE Transactions on Signal Processing, 51, 442–457.
[44] Lisowska A.: Nonlinear Weighted Median Filters in Dyadic Decomposition of Images. Annales UMCS Informatica AI, 1, 157–164.
[45] Prieto M. S., Allen A. R.: A Similarity Metric for Edge Images. IEEE Transactions on Pattern Analysis and Machine Intelligence, 25(10), 1265–1273.

[46] Romberg J., Wakin M., Baraniuk R.: Multiscale Geometric Image Processing. SPIE Visual Communications and Image Processing, Lugano, Switzerland.

[47] Yitzhaky Y., Peli E.: A Method for Objective Edge Detection Evaluation and Detector Parameter Selection. IEEE Transactions on Pattern Analysis and Machine Intelligence, 25(8), 1027–1033.

[48] Zhang J. K., Davidson T. N., Wong K. M.: Efficient design of orthonormal wavelet bases for signal representation. IEEE Transactions on Signal Processing.

2004

[49] Lisowska A., Porwik P.: New Extended Wavelet Method of 2D Signal Decomposition Based on Haar Transform. Mathematics and Computers in Simulation, Elsevier Journal, (to appear).

[50] Porwik P., Lisowska A.: The New Graphic Description of the Haar Wavelet Transform. Lecture Notes in Computer Science, Springer–Verlag, Berlin, Heidelberg, New York, 3039, 1–8.